Effects of Mixed Solvent on Gelation of Poly(vinyl alcohol) Solutions

PO-DA HONG, CHE-MIN CHOU, WEI-TSUNG CHUANG

Department of Textile and Polymer Engineering, National Taiwan University of Science and Technology, Taipei 10607, Taiwan, Republic of China

Received 13 January 1999; accepted 8 March 2000

ABSTRACT: The relationship between the polymer–solvent interaction and gelation behavior of poly(vinyl alcohol) (PVA) solutions prepared from ethylene glycol/water (EG/water) mixed solvents was investigated using a viscometer, light scattering, FTIR, X-ray, and pulsed NMR analyses. The viscometric result showed that the affinity to PVA for water is higher than that for EG. The light scattering result showed that the spinodal decomposition rate of the PVA solution decreases rapidly as the water content in the EG/water mixed solvent is increased. On the other hand, the FTIR and X-ray results both indicated that the crystallinity of the PVA gel decreases with water content. These results imply that the water molecules must improve the affinity of the solvent to PVA to inhibit the aggregation or crystallization of PVA chains. The pulsed NMR measurement results showed that the spin–spin relaxation times related to the polymer-rich and polymer-poor phases of the PVA gel increase, and the fractional amount of the polymer-poor phase increases while that of the polymer-rich phase decreases with increasing water content. These facts indicated that the increase in the mobility of PVA chains must give rise to the difficulty in chain aggregation of PVA solutions with increasing water content. Two transition temperatures were found in the phase transition of the polymer-rich phase. The lower transition temperature was attributed to the destruction of the denser chain entanglements in the polymer-rich phase and the higher transition temperature was mainly concerned with the melting of the crystallites. © 2000 John Wiley & Sons, Inc. J Appl Polym Sci 79: 1113–1120, 2001

Key words: poly(vinyl alcohol); interaction; gelation; mixed solvent; pulsed NMR

INTRODUCTION

Poly(vinyl alcohol) (PVA) gel is a well-known crystallization-induced physical gel, and the studies on these PVA gels attract much interest because the relationship between polymer–solvent interaction and the physical properties of gels is very complicated. Many researchers[1–8] already reported that PVA solutions can form gels in various kinds of solvents. Ohkura et al.[1,2] reported that highly elastic PVA gels prepared from DMSO/water mixed solvents below −20°C are transparent, and their gelation rate is very fast compared with those prepared from aqueous solutions. In our previous studies,[9,10] PVA gels from ethylene glycol (EG) and *N*-methyl-2-pyrrolidinone (NMP) solvents showed that the average size of the crystallite in a PVA/EG gel is larger than that in a PVA/NMP gel (i.e., the aggregation of PVA chains occurs more easily in the poor solvent, EG, than in the good solvent, NMP). Recently, Matsuo et al.[11,12] studied the phase separation behavior of PVA/DMSO/water mixed solu-

Correspondence to: P.-D. Hong (phong@hp730.tx.ntust.edu.tw).

Contract grant sponsor: National Science Council of Republic of China; contract grant number: NSC-87-2216-E011-005.

Journal of Applied Polymer Science, Vol. 79, 1113–1120 (2001)

tions and indicated that the logarithm of the scattered intensity in the light scattering from PVA solutions increased linearly with time at the initial stage of the phase separation. The phase separation occurred rapidly where the water content in the mixed solvent was about 30–50 vol %.

The phase transitions in the polymer gels were also investigated by NMR.[13,14] Ohta et al.[13] reported on the effect of hydrostatic pressure on the gelation of an aqueous solution of poly(*N*-isopropylacrylamide) (NIPA). A sudden shortening of the spin–spin relaxation time (T_2) of the polymer chains in solution was observed during gelation, implying that the chain mobility slowed down where the polymer chains started to aggregate to form the network structure. Tokuhiro et al.[14] also presented the near phase transition of NIPA gels by using the pulsed NMR technique. They showed that NIPA gels undergo continuous second-order volume phase separation or discontinuous first-order transitions in response to the temperature change.

In this work the change of the polymer–solvent interaction with the composition of the solvent used was first investigated through a viscometric measurement, then the liquid–liquid phase behavior of PVA solutions from the results of the time-resolved light scattering measurement was discussed. Finally, the pulsed NMR analysis was used to investigate the degree of aggregation and the phase transition of PVA gels prepared from the solutions with various solvent compositions.

EXPERIMENTAL

Samples

PVA powder (weight-average molecular weight = 155,000, Aldrich) with a high degree of hydrolysis (about 99.8%) was used in this work. The mixed solvents with various compositions of EG and water were used to prepare PVA solutions. The homogeneous PVA solutions with various PVA concentrations were obtained by heating them at 90–130°C for 2 h and then cooling to room temperature for gelation. For light scattering measurement the solutions were filtered directly into a light scattering cell using 0.45 or 1.0μm Millipore filters.

Measurements

Determination of the viscosity of the dilute PVA solution was carried out with an Ubbelohde viscometer immersed in a thermostatic water bath held at 30 ± 0.1°C for 1 h. The intrinsic viscosity [η] was obtained using the Huggins equation[15]:

$$(t - t_o/t_o)/C = (\eta_{sp}/C) = [\eta] + k'[\eta]^2C \quad (1)$$

where t is the flow time of the dilute solution, t_o is the flow time of the pure solvent, C is the concentration of the polymer, η_{sp} is the specific viscosity, and k' is the Huggins constant.

An "upside-down test-tube" method was used to determine the gel melting point (T_m^G) of the PVA gels prepared from various compositions of mixed solvents. The sealed test tube with gel was kept upside down in a thermostat oven and it was heated at a rate of 1°C/min to evenly heat the gel in the test tube. The temperature at which the gel began to flow was defined as the T_m^G of the gel.

The IR spectra were measured by using Digilab Division Bio-Rad spc-3200 FTIR equipment. The peaks at 1141 and 1095 cm^{-1} were assigned to the transmittance of the crystalline and the amorphous sequences, respectively.[16,17] The transmittance ratio of 1141/1095 cm^{-1} is the regularity index of the PVA gel.

The wide angle X-ray intensity curves of the gels were measured with graphite-monochromatized CuKα radiation generated at 40 kV and 100 mA in a Rigaku D/max diffractometer at a scanning speed of 2θ = 1°/min.

Elastic light scattering measurements were carried out with a Malvern series 4700 apparatus; the light source was a 2-W argon ion laser operating at a power of 100 mW and a wavelength of 514.5 nm with vertically polarized light, which was focused on the sample cell through a temperature-controlled chamber (the temperature being controlled to within ±0.1°C) filled with distilled water. The scattering vector of the light scattering was $q = (4n\pi/\lambda)\sin(\theta/2)$, where θ is the scattering angle and n is the refractive index of the medium. The change of the scattered intensity with time during the isothermal phase separation was measured at θ = 90°.

Pulsed H^1-NMR measurements were carried out using a Maran-20 pulsed NMR spectrometer operating at a fixed frequency of 20 MHz. The recovery time of the spectrometer following a sequence of pulses was 13 μs. The T_2 measurements were carried out using the Carr–Purcell–Meiboom–Gill (CPMG) pulsed sequence[18] $[90°_x\tau(180°_y2\tau)_n]$ (P90° = 2.8 μs, P180° = 5.6 μs, and n = 4096) available for a long T_2 sample, for example, the wet gel system, to eliminate the effect of heterogeneity in the static magnetic field.

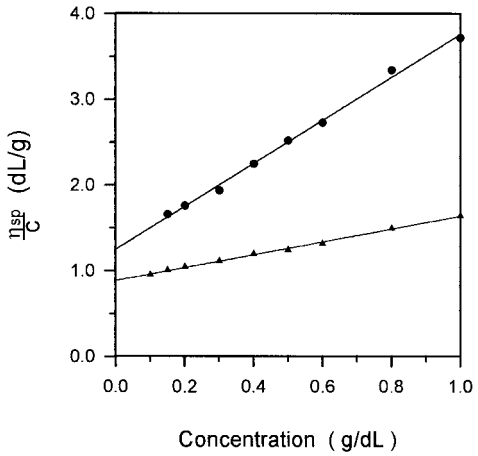

Figure 1 A plot of the η_{sp}/C versus C for PVA dilute solutions: (●) PVA/EG solution and (▲) PVA/water solution.

RESULTS AND DISCUSSION

Figure 1 shows the η_{sp}/C versus C plot for pure PVA/EG and PVA/water dilute solutions. From the linear relationship in Figure 1, the k' could be obtained using eq. (1). Sakai[19,20] reported that the k' value for a polymer solution at the θ condition is about 0.52, and in a good solvent the k' value should be less than 0.52. Therefore, a solution with a lower k' value (<0.52) is considered to be a good solvent, which means a higher solubility and strongly attractive interaction between the polymer and solvent. The calculated result showed that the k' values for PVA/EG and PVA/water solutions are about 1.53 and 0.49, respectively. This means that the affinity to PVA for water is higher than that for EG. Andreyeva et al.[21] pointed out that only the use of solvents such as diols and triols have made it possible to form a single crystal from the dilute PVA solutions. Rogovina et al.[22] also determined the thermodynamic quality of the solvent by light scattering and ultracentrifugation methods. Their results also indicated that the second virial coefficient (A_2) of PVA/water was higher than that of PVA/glycerin. These facts may imply that the crystallization in PVA solutions with poorer solvents proceeds much more easily. The manner in which the properties of PVA in mixed solvents affects the aggregation behavior of PVA chains is discussed in this study.

Measurements of the time dependence of the intensity of light scattering from a polymer solution could provide information about the kinetics of spinodal decomposition or the liquid–liquid phase separation of the solution. The rate of spinodal decomposition or the liquid–liquid phase separation can be easily obtained according to the Cahn–Hilliard–Cook[23–25] theory at the early stage of spinodal decomposition. Pines and Prins[26] applied the concept of spinodal decomposition to the gelation process and interpreted the origin of network structure in terms of the connectivity of the polymer-rich phase. Matsuo et al.[27,28] also studied the phase separation behavior of PVA/DMSO/water solutions through the elastic light scattering technique and showed that the logarithm of the scattered intensity from the PVA solution increased linearly with time in the initial stage of phase separation. Figure 2 shows the logarithm of the scattered intensity as a function of time for PVA solutions with various water contents at $\theta = 90°$. Although the time at which the spinodal decomposition starts differs for each of the various PVA solutions, the logarithm of the scattered intensity increases linearly with time for the solution, which undergoes the liquid–liquid phase separation. The phase separation of pure PVA/EG solution is very fast; therefore, the scattered intensity increases rapidly and reaches equilibrium. The linear theory of the spinodal decomposition mechanism at the initial stage of phase separation was proposed by Cahn–Hilliard–Cook[23–25], which is given as follows:

$$I(q, t) = I(q, t = 0)\exp[2R(q)t] \qquad (2)$$

where $I(q, t)$ is the scattered intensity at time t after initiation of the spinodal decomposition and

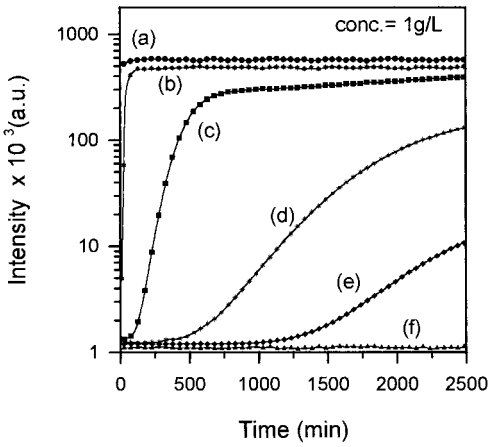

Figure 2 A plot of the logarithm of the scattered intensity at $\theta = 90°$ as a function of time at 30°C. The water content in the mixed solvent was (a) 0, (b) 10, (c) 20, (d) 30, (e) 40, and (f) 50 vol %.

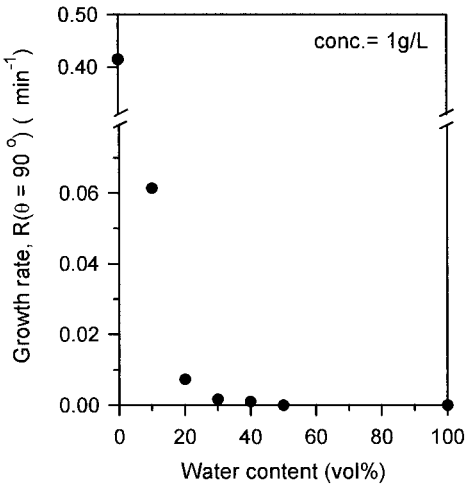

Figure 3 The plot of the growth rate of the concentration fluctuation [$R(\theta = 90°)$] as a function of the water content.

$R(q)$ is the growth rate of the concentration fluctuation given as a function of q. Although eq. (2) shows the $R(q)$ value changes with q, the only $R(\theta = 90°)$ value is presented as a reference for the qualitative discussion in this work. According to the linear theory described by eq. (2), a plot of $\ln(I)$ versus t should yield a straight line of the slope $2R(q)$. Figure 3 shows the $R(\theta = 90°)$ value as a function of the water content in the EG/water mixed solvent. The $R(\theta = 90°)$ value is rapidly reduced at 10 vol % water content and then decreases slowly with increasing water content, implying that the thermodynamic driving force for the easily reduced liquid–liquid phase separation must be the water molecules. The proceeding of the spinodal decomposition induced by the thermodynamic driving force of the liquid–liquid phase separation is difficult because of the stronger polymer–solvent interaction. The $R(\theta = 90°)$ value approaches zero at a water content higher than 50 vol %, indicating that the chain aggregation of the PVA solution became very difficult under this condition in this work.

Figure 4 shows the scattered profiles [$I(\theta)$ vs. θ] after the initiation of the liquid–liquid phase separation of PVA solutions as a function of the water content. The appearance of a distinct scattering maximum is considered to be due to the phase separation or the chain aggregation of the polymer solution.[26–28] The scattering peak position shifts to a larger angle region with increasing water content. This is because the size of the aggregating clusters becomes smaller (i.e., it is more difficult for the phase separation of the PVA solution to proceed as the water content is increased). Andreyeva et al.[21] studied the phase diagrams of PVA/EG and PVA/water solutions and indicated that the phase diagram of the PVA/EG solution exhibited the characteristic of "crystalline" separation, while the characteristic of an "amorphous" phase separation diagram was found in the aqueous PVA solution. This fact also implies that there is a water content affect on the aggregation behavior of PVA/EG/water mixed solutions.

Physical gel systems often exhibit a heterogeneous structure,[10,29–34] which leads to the heterogeneity in the molecular mobility with a multiexponential decay of transverse magnetization in pulsed NMR. The decaying signals of transverse magnetization [$M(t)$] for the polymer gel system are expressed empirically as the following Weibull function[35]:

$$M(t) = M_0 \exp[-(1/a)(t/T_2)^a] \quad (3)$$

where M_0 is a constant proportional to the total number of nuclei with magnetic moments and t is the decaying time. The a value is the shape parameter, $1 \leq a \leq 2$, which could express the characteristics of the different components. For $a = 1$ the T_2 value can be disposed to the mobile component or the polymer-poor phase in the gel, and for $a = 2$ the T_2 can be disposed to the immobile component or the polymer-rich phase in the gel. The nonlinear least-squares method that fits the experimental data into the following equa-

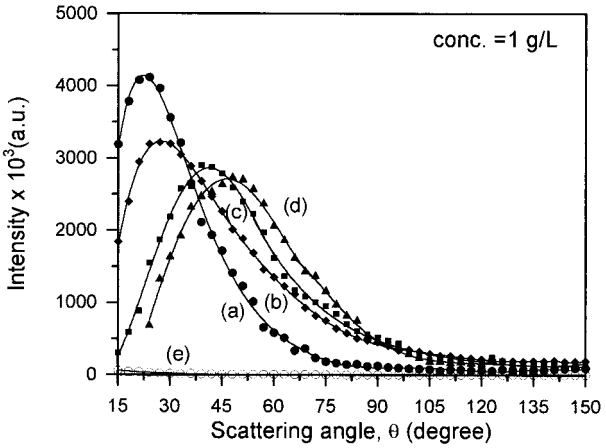

Figure 4 The scattered profiles [$I(\theta)$ vs. θ] of PVA solutions ($C = 1$ g/L) aged for 2 days at 30° as a function of water contents of (a) 0, (b) 10, (c) 20, (d) 30, and (e) 50 vol %.

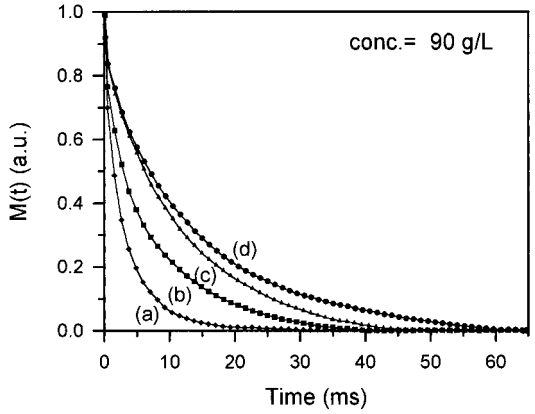

Figure 5 The decaying signals of CPMG for PVA gels at 30°C as a function of water contents of (a) 0, (b) 20, (c) 30, and (d) 40 vol %.

tion makes the analysis of the decaying process as follows:

$$M(t) = M_{0A}\exp\left\{-\frac{1}{2}(t/T_{2A})^2\right\} + M_{0B}\exp(-t/T_{2B}) \quad (4)$$

where M_{oi} is the magnetic moment of the ith component and T_{2i} is the T_2 of the ith component. From this fitting procedure the decaying signals of the PVA gels were roughly decomposed into two components. The fast decaying signals were from the chain mobility in the immobile/polymer-rich component related to the crystallite and the denser chain aggregation, and the slow decaying ones were from that in the mobile/polymer-poor component related to the flexible chain connected between the junction points and the free solvent molecules. The fractional amount f of each component is obtained from $f^S = [M_{0A}/M(t)] \times 100\%$ and $f^L = [M_{0B}/M(t)] \times 100\%$ for the polymer-rich and polymer-poor components, respectively. Ohta et al.[13] reported on the effect of hydrostatic pressure on the gelation in an aqueous solution of NIPA. They indicated a sudden shortening of the T_2 of the aqueous solution observed during gelation, implying the slowing down of the mobility of the polymer chains. Tokuhiro et al.[14] also presented an NMR study of the phase transition in NIPA gels. They reported that the NIPA gels undergo continuous second-order volume phase separation or discontinuous first-order transitions in response to temperature change. Our previous study[34] also reported that the increase in the degree of chain aggregation and the number of junction points for a poly(vinyl chloride)/dioxane (PVC/DOA) gel resulted in the reduction of the chain mobility of the PVC/DOA gels. The T_2 values for the polymer-rich (T_2^S) and polymer-poor (T_2^L) phases in the PVC/DOA gel decreased with increasing molecular weight and concentration of the polymer. These facts are considered in relation to the polymer chains associating with each other in forming the polymer-rich region to reduce chain mobility in the gel.

Figure 5 shows the typical decaying signals of CPMG for PVA gels with various water contents. The CPMG signals decayed to a longer time region as the water content was increased. The decaying signals of the gels were roughly decomposed into two components using eq. (4). Figure 6 shows the T_2 and f values of two components, which were obtained from the CPMG decaying signals for various PVA samples as a function of the water content at 30°C. The component with longer the T_2, T_2^L, originated from the mobile domain/polymer-poor phase and the component with shorter the T_2, T_2^S, originated from the immobile domain/polymer-rich phase. In Figure 6 the T_2^S and T_2^L values of the PVA samples both rise with increasing water content. At the water content above 50 vol %, the samples only exhibit a T_2^L value, indicating that the samples are still a homogeneous solution without any larger chain aggregation. Regarding the results in the gel state (water content below 50 vol %), the increase in the T_2^S value with the water content must be due to the change of the chain mobility in the polymer-rich phase. This is because the affinity of the solvent to PVA increases with the water con-

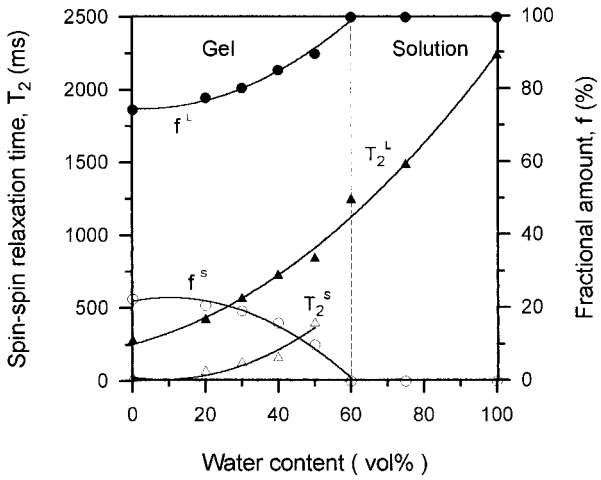

Figure 6 The spin–spin relaxation time (T_2) and the fractional amount (f) from CPMG signals of each component for PVA samples (C = 90 g/L) as a function of the water content: (△) T_2^S, (▲) T_2^L, (○) f^S, and (●) f^L.

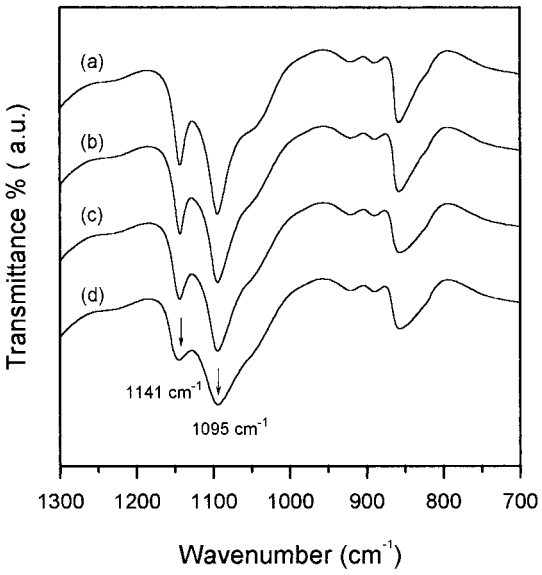

Figure 7 FTIR spectra of PVA gels (C = 90 g/L) as a function of water contents of (a) 0, (b) 10, (c) 20, and (d) 30 vol %.

tent, resulting in the difficult liquid–liquid phase separation (i.e., the packing density of chain aggregation becomes less, leading to an increase in the chain mobility in the polymer-rich phase). On the other hand, the increase in the T_2^S value must also be due to the PVA chains in the polymer-poor phase becoming more soluble, which leads to an increase in the chain mobility. Because of the various interactions between the polymer and solvent in the PVA solutions, the degree of chain aggregation of PVA samples must also be reflected in the change of the f^L and f^S values in Figure 6. As mentioned above, the gelation of the PVA solution could not occur above the 50 vol % water content at 30°C (i.e., the f^S value approaches zero at this condition). This means that the samples should still be homogeneous solutions or sols without any significant chain aggregation. In the gel state the f^L value gradually increased and f^S value decreased with water content.

Figure 7 shows the FTIR spectra of PVA gels prepared from the same gelation condition as in Figure 5. The peaks at 1141 and 1095 cm^{-1} were assigned to the crystalline and amorphous sequences, respectively. Therefore, the transmittance ratio of 1141/1095 cm^{-1} was considered to be the regularity index of the PVA chain. The transmittance ratio of 1141/1095 cm^{-1} for the PVA gel changed significantly as the water content was increased. The crystallite absorption peak (1141 cm^{-1}) showed a remarkable decrease with increasing water content, indicating that the crystallinity of the gel became lower with the water content. On the other hand, Figure 8 shows X-ray intensity curves of PVA gels as a function of the water content. Although a large part of the intensity was the contribution of the solvents, the (101) diffraction peak of the PVA crystal clearly appeared at about 2θ = 19°. It should be noted that the (101) diffraction of th ePVA crystal was due to the intermolecular interference between the PVA chains in the direction of the intermolecular hydrogen bonding. Therefore, the increase in the intensity of the (101) diffraction corresponded to the increase in the number of the regular PVA chains packing together. The decrease in the (101) diffraction intensity with the water content indicated that the size of the PVA crystallite in the gel network became smaller because of the difficulty of the crystallization.

Figure 9 shows the variation in the f^S value with the temperature change from 20 to 150°C for various PVA gels. These could be divided into three regions from the results of the temperature dependence of the f^S value. The plot exhibited two transition points in the polymer-rich phase. The phase transition in the PVA gel could be classified into three regions as shown in Figure 9. The gels obviously changed their appearance with the temperature in these three regions. Region I showed a harder PVA gel with an opaque or turbid appearance. As the temperature reached region II, the sample became a soft and transparent gel. Finally, the PVA gel began to flow above the higher transition temperature in region III. Generally, it is considered that the polymer-rich

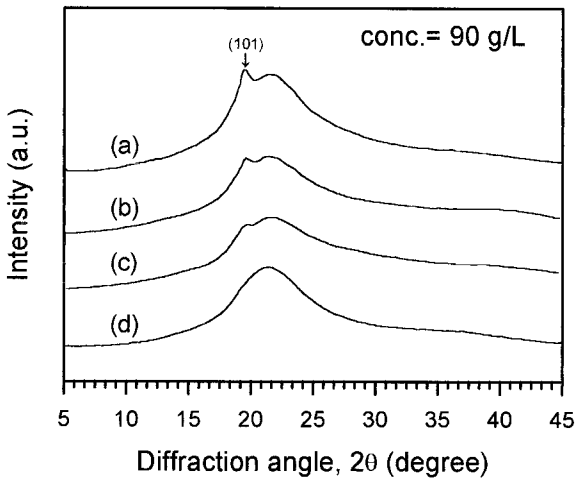

Figure 8 X-ray intensity curves of PVA gels (C = 90 g/L) as a function of water contents of (a) 0, (b) 10, (c) 20, and (d) 30 vol %.

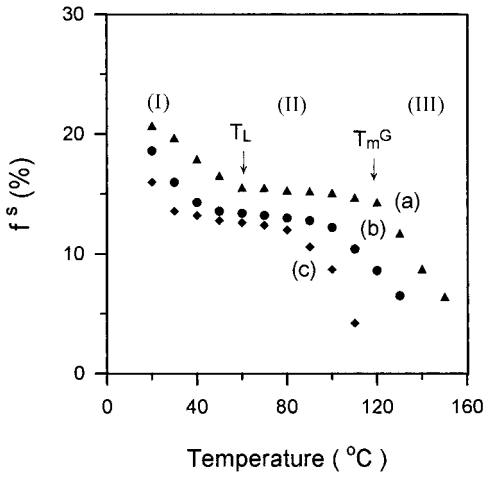

Figure 9 The dependence of the temperature on the fractional amount in the polymer-rich phase (f^S) for PVA gels (C = 90 g/L) as a function of water contents of (a) 0, (b) 20, and (c) 40 vol %.

phase consists of denser chain aggregation and crystallites. Therefore, the lower transition temperature (T_L) must be related to the destruction of denser chain entanglements in the polymer-rich phase and the higher transition temperature (T_m^G) is mainly concerned with the melting of the crystallites.

Figure 10 shows the T_m^G values obtained from the pulsed NMR and upside-down test-tube methods and the T_L as a function of the water content. The T_m^G and T_L values both decreased with increasing water content. Besides, two T_m^G values were in good agreement, irrespective of the various estimation methods. Generally, the T_m^G determined from the upside-down test-tube method is defined as the temperature at which the gel begins to flow. Because the microcrystallites play the role of the junctions in the gel network, the T_m^G must be mainly related to the melting of PVA crystals. In our previous study[10] we considered that the significant crystallization of PVA/EG solution must take place for the gelation because of the poor solubility of the solvent, then resulting in an opaque gel with high crystallinity. Stokes and Berghmans[6] also proposed an aggregation model for the gelation mechanism of PVA/EG solution through thermal and X-ray analyses. Their model indicated that the PVA/EG gel prepared at room temperature consists of some particle-like aggregates (polymer-rich phase) as physical crosslinks in which many crystallites are present. As the water content in the mixed solvent is increased, the affinity of the solvent to PVA must be increased to give rise to the lower thermal resistance of the gel. In this work we observed that the opaque PVA/EG gel became gradually turbid or translucent as the water was added into the EG. A thinner gel network must be formed because of less chain aggregation in PVA/EG/water systems.

CONCLUSIONS

The effects of polymer–solvent interaction on the aggregation behavior and phase transition of PVA/EG/water gels were studied. The viscosity result of diluted PVA solutions showed that the Huggins constants for pure PVA/EG and PVA/water solutions were about 1.53 and 0.49, respectively. This meant that the PVA affinity for water is higher than that for EG. The solvent effect on the aggregation behavior of PVA solutions was investigated through light scattering measurement. The linear increase in the logarithm of the scattered intensity with time was believed to be described by the linear theory of spinodal decomposition at the initial phase separation. The rate of spinodal decomposition of the PVA solution was rapidly reduced at 10 vol % water content and then gradually decreased with increasing water content, implying that the thermodynamic driving force for the liquid–liquid phase separation must be easily reduced because of the water molecules. The spinodal decomposition induced by the thermodynamic driving force of the liquid–liquid phase separation was difficult because of the stronger polymer–solvent interaction. The ap-

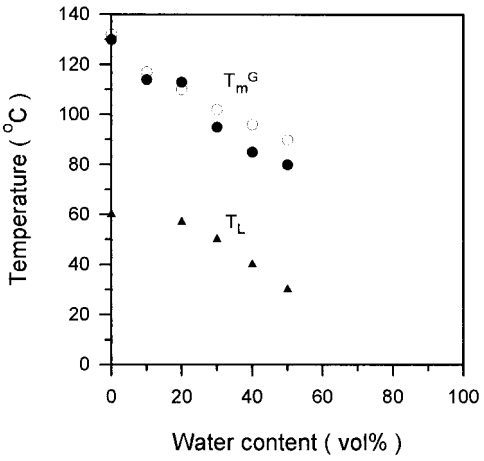

Figure 10 A plot of the transition temperature as a function of the water content. (●) T_m^G and (△) T_L are the high and low transition temperatures in Figure 9, respectively; (○) T_m^G is determined from the upside-down test-tube method.

pearance of a distinct scattering maximum in the scattered profile [$I(\theta)$ vs. θ] was considered to be attributable to the phase separation and chain aggregation of the polymer solution. The scattering peak position shifted to a larger angle region, indicating that the chain aggregation became smaller with increasing water content. This result was in agreement with FTIR and X-ray results in gels that showed the crystallinity decreased as the water content in the mixed solvent was increased. The pulsed NMR results showed that the T_2^S, T_2^L, and f^L of the PVA gel increased while the f^S decreased as the water content in the mixed solvent increased. At the water content above 50 vol %, the samples only exhibited a T_2^L value, indicating that the samples were still homogeneous solutions without any larger chain aggregation. The increase in the T_2^S value with the water content must have been due to the increase in the affinity of the solvent, to PVA, resulting in the difficult liquid–liquid phase separation (i.e., less packing density of the chain aggregate increased the chain mobility in the polymer-rich phase). Two transition temperatures were found in the phase transition of the polymer-rich phase. The lower transition temperature was considered to be due to the destruction of denser chain entanglements in the polymer-rich phase, and the higher transition temperature was mainly concerned with the melting of crystallites.

REFERENCES

1. Ohkura, M.; Kanaya, T.; Kaji, K. Polymer 1992, 33, 3689.
2. Ohkura, M.; Kanaya, T.; Kaji, K. Polymer 1992, 33, 5044.
3. (a) Watase, M.; Nishinari, K. Polymer J 1989, 21, 567; (b) Watase, M.; Nishinari, K. Polymer J 1989, 21, 597.
4. Yamaura, K.; Katoh, H.; Tanigami, T.; Matsuzawa, S. J Appl Polym Sci 1987, 34, 2347.
5. Cebe, P.; Grubb, D. J Mater Sci 1985, 20, 4465.
6. Stokes, W.; Berghmans, H. Brit Polym J 1988, 20, 316.
7. Nishinari, K.; Watase, M. Polym J 1993, 25, 463.
8. Hyon, S. H.; Cha, W. L.; Ikada, Y. Polym Bull 1989, 22, 119.
9. Hong, P. D.; Miyasaka, K. Polymer 1991, 32, 3140.
10. Hong, P. D.; Chen, J. H.; Wu, H. L. J Appl Polym Sci 1998, 69, 2477.
11. Matsuo, M.; Sudiura, Y.; Takematsu, S.; Ogita, T.; Sakabe, T.; Nakamura, R. Polymer 1997, 38, 5953.
12. Matsuo, M.; Kawase, M.; Sudiura, Y.; Takematsu, S.; Hara, C. Macromolecules 1993, 26, 4461.
13. Ohta, H.; Ando, I.; Fujishige, S.; Kubota, K. In Proceedings of the 3rd Symposium on Polymer Gels, Japan, 1990; p 7.
14. Tokuhiro, T.; Amiya, T.; Mamada, A.; Tanaka, T. Macromolecules 1991, 24, 2936.
15. Sperling, L. H. Introduction to Physical Polymer Science; Wiley: New York, 1986; p 78.
16. Finch, C. A. Polyvinyl Alcohol—Developments; Wiley: New York, 1992.
17. (a) Papkov, S. P.; Yefimova, S. G.; Shablygin, M. V.; Mikhailov, N. V. Vysokomol Soyed 1966, 8, 1035; (b) Papkov, S. P.; Yefimova, S. G.; Shablygin, M. V.; Mikhailov, N. V. Polym Sci USSR 1966, 8, 1135.
18. Meiboom, S.; Gill, D. Rev Sci Instrum 1958, 29, 688.
19. Sakai, T. J Polym Sci A-2 1968, 6, 1535.
20. Sakai, T. Macromolecules 1970, 3, 96.
21. (a) Andreyeva, V. M.; Anikeyeva, A. A.; Lirova, B. I.; Tager, A. A. Vysokomol Soyed (A) 1973, 15, 1770; (b) Andreyeva, V. M.; Anikeyeva, A. A.; Lirova, B. I.; Tager, A. A. Polym Sci USSR 1973, 15, 1991.
22. (a) Rogovina, L. Z.; Slonimskii, G. L.; Gembitskii, L. S.; Serova, Y. A.; Grigor'eva, V. A.; Gubenkova, Y. N. Vysokomol Soyed (A) 1973, 15, 1256; (b) Rogovina, L. Z.; Slonimskii, G. L.; Gembitskii, L. S.; Serova, Y. A.; Grigor'eva, V. A.; Gubenkova, Y. N. Polym Sci USSR 1973, 15, 1411.
23. Cahn, J. W. J Chem Phys 1965, 42, 93.
24. Cahn, J. W.; Hilliard, J. E. J Chem Phys 1958, 1958, 28, 258.
25. Cook, H. E. Acta Metall 1970, 18, 297.
26. Pines, E.; Prins, W. Macromolecules 1973, 6, 888.
27. Sawatari, C.; Yamamoto, Y.; Yanagida, N.; Matsuo, M. Polymer 1993, 34, 956.
28. Matsuo, M.; Sugiura, Y.; Takematsu, S.; Ogita, T.; Sakabe, T.; Nakamura, R. Polymer 1997, 38, 5953.
29. Ikehara, T.; Nishi, T.; Hayashi, T. Polym J 1996, 28, 169.
30. Shiga, T.; Fukumopi, K.; Hirose, Y.; Okada, A.; Kurauchi, T. J Polym Sci Polym Phys Ed 1994, 32, 85.
31. Tanaka, H.; Nishi, T. Phys Rev B 1986, 33, 32.
32. Fukumori, K.; Kurauchi, T.; Kamigaito, O. Polymer 1990, 31, 713.
33. Fukumori, K.; Kurauchi, T.; Kamigaito, O. J Appl Polym Sci 1989, 38, 1313.
34. Hong, P. D.; Chen, J. H. Polymer 1998, 39, 5809.
35. Kaufman, S.; Slichter, W. P.; Davis, D. D. J Polym Sci A-2 1971, 9, 829.